A Pre-Steady State Analysis of Ligand Binding to Human Glucokinase: Evidence for a Preexisting Equilibrium

Young B. Kim,[‡] Stephen S. Kalinowski,[§] and Jovita Marcinkeviciene*,[‡]

Departments of Chemical Enzymology and Metabolic Diseases, Bristol Myers-Squibb Pharmaceutical Company, Pharmaceutical Research Institute, P.O. Box 5400, Princeton, New Jersey 08543-5400

Received August 23, 2006; Revised Manuscript Received October 23, 2006

ABSTRACT: Cooperativity with glucose is a key feature of human glucokinase (GK), allowing its crucial role as a glucose sensor in hepatic and pancreatic cells. We studied the changes in enzyme intrinsic tryptophan fluorescence induced by binding of different ligands to this monomeric enzyme using stopped-flow and equilibrium binding methods. Glucose binding data under pre-steady state conditions suggest that the free enzyme in solution is in a preexisting equilibrium between at least two conformers (super-open and open) which differ in their affinity for glucose (K_d* = 0.17 ± 0.02 mM and K_d = 73 ± 18 mM). Increasing the glucose concentration changes the ratio of the two conformers, thus yielding an apparent K_d of 3 mM (different from a K_m of 7−10 mM). The rates of conformational transitions of free and GK complexed with sugar are slow and during catalysis are most likely affected by ATP binding, phosphate transfer, and product release steps to allow the k_{cat} to be 60 s^{-1}. The ATP analogue PNP-AMP binds to free GK (super-open) and GK−glucose (open) complexes with comparable affinities (K_d = 0.23 ± 0.02 and 0.19 ± 0.08 mM, respectively). However, cooperativity with PNP-AMP observed under equilibrium binding conditions in the presence of glucose (Hill slope of 1.6) is indicative of further complex tightening to the closed conformation. Another physiological modulator (inhibitor), palmitoyl-CoA, binds to GK with similar characteristics, suggesting that conformational changes induced upon ligand binding are not restricted by an active site ligand. In conclusion, our data support control of GK activity and K_m through the ratio of distinct conformers (super-open, open, and closed) through either substrate or other ligand binding and/or dissociation.

Glucokinase (hexokinase D, often known as hexokinase IV, EC 2.7. 1.1) is one of the four glucose-phosphorylating isoenzymes present in mammals and plays the role of a glucose sensor in pancreatic β-cells and hepatocytes (*1*). The significance of glucokinase in the control of blood glucose is underscored by data from transgenic animals, in which GK[1] activity has been modulated, and in humans, possessing enzyme mutations. Pancreatic or liver-specific GK knockout mice display hyperglycemia (*2*), while overexpression of GK in mice leads to lower fasting blood glucose levels and resistance to the development of high-fat diet-induced diabetes (*3*, *4*). In humans, naturally occurring inactivating and activating mutations in the glucokinase gene were reported to cause maturity onset diabetes of the young type 2 (MODY2) (*5*, *6*) and persistent hyperinsulinemic hypoglycemia of infancy (PHHI) (*7*), respectively. These data, taken together, illustrate the importance of the GK in regulating glucose homeostasis and suggest that pharmacological activation of this enzyme in type 2 diabetes patients could have clinical benefits.

In recent years, several groups have reported the discovery of small molecules which enhance glucokinase activity by binding at an allosteric site. These compounds stimulate insulin secretion in a glucose-dependent manner in pancreatic β-cells and increase the level of glucose use in rat hepatocytes. Activators lowered blood glucose levels and improved glucose tolerance tests in wild-type and diet-induced obese mice (DIO) (*8*−*10*).

The sigmoidal glucose saturation curve, an unusual property for a monomeric enzyme, allows glucokinase to perfectly serve its biological function as a glucose sensor. Models that account for the cooperative kinetic behavior of glucokinase assume the existence of two different conformations with different affinities that interconvert slowly, thus allowing glucose to increase the proportion of the conformation with a higher affinity (*11*, *12*). A recently determined crystal structure of inactive (ligand-free) and activated (with glucose and an allosteric small molecule bound) human glucokinase demonstrated a global domain reorganization upon ligand binding which could account for a slow step and cooperativity (*13*).

Glucokinase cooperativity is a desirable kinetic property, and understanding how different ligands impact it could provide a novel framework in the search for useful pharmacological agents. In this work, we describe pre-steady state and equilibrium binding methods for following how different

* To whom correspondence should be addressed. Phone: (609) 818-5197. Fax: (609) 818-6935. E-mail: jovita. marcinkeviciene@bms.com.
[‡] Department of Chemical Enzymology.
[§] Department of Metabolic Diseases.

[1] Abbreviations: GK, glucokinase; PNP-AMP, adenosine 5′-(β,γ-imido)triphosphate; NAG, *N*-acetyl-D-glucosamine.

10.1021/bi0617308 CCC: $37.00
Published on Web 01/11/2007

ligands (substrates and inhibitors) affect conformational transitions in glucokinase.

MATERIALS AND METHODS

Expression and Purification of Human GK. Full-length human hepatic GK (untagged) was expressed in BL21 STAR (DE3)pLysS cells (Invitrogen) at 25 °C as described by Mookhtiar et al. (*14*). The protein was purified essentially as described previously (*15*) with slight modification. Briefly, cell pellets were lysed via three rounds of freezing and thawing, centrifuged at 15000*g* for clarification, and precipitated with 40−65% $(NH_4)_2SO_4$. The resulting pellet was resuspended in buffer, dialyzed, and applied directly to a Q-Sepharose (Sigma) column following the elution as described earlier. The most active fractions were applied to a high-resolution Tricorn MonoQ (10/100 GL) column (GE Healthcare), and the protein was eluted with a linear 0 to 1 M NaCl gradient. The activity eluted in two very well resolved peaks (a major peak at 350 mM NaCl and a minor peak at 400 mM NaCl) which were identical in their specific activity, kinetics, and behavior on the SDS protein gel. Our final enzyme solution was a mixture of both fractions. The major fraction separately exhibited kinetic properties identical to those of the mixture.

Stopped-Flow Binding Studies. Rapid kinetic studies were performed using an Applied Photophysics SX18MV stopped-flow spectrofluorometer with excitation at 285 nm. The instrument was set with a 2 mm path length cell and excitation band of <10 nm. The emission intensity was monitored through a cutoff filter (WG-320 nm) installed in front of the photomultiplier. The dead time of the instrument was 1.2 ms. Experiments were performed under pseudo-first-order conditions by mixing equal volumes of the enzyme (final concentration of 1 μM) and ligand in 25 mM Hepes, 1 mM DTT, and 5 mM $MgCl_2$ (pH 7.1). In the cases in which precomplexed enzyme was studied, excess ligand was included in both syringes (to compensate for dilution effects), but only one contained the variable second ligand. Rate constants (k_{obs} from the fits to single- or double-exponential equations) were determined from five to eight runs under each condition. Values of k_{obs} as a function of the ligand concentration were then fit to the specific mechanism as shown below.

Equilibrium Binding Studies. Intrinsic tryptophan fluorescence changes at equilibrium were monitored using a Hitachi F-2500 fluorescence spectrophotometer. Samples were excited at 285 nm and emission spectra collected from 290 to 400 nm. Ligand titrations involved 1 μL additions to a 1 mL glucokinase solution (1 μM) in 25 mM Hepes with 1 mM DTT and 5 mM $MgCl_2$ (pH 7.1). All emission values were corrected for dilution. Palmitoyl-CoA titrations were performed in buffer without $MgCl_2$ to minimize potential micelle formation (*16*).

Data Analysis. The change in the fluorescence signal under the pre-steady state conditions was related to the transition of one enzyme species (E) to another (either E*L or EL+E*L) upon ligand binding. In the experiments where the transient could be fit to a single-exponential equation, we assumed that only one enzyme form yielded a fluorescence signal or multiple forms with the same quantum yield. The signal change in time at one concentration of the ligand was defined by k_{obs}. In the experiments in which k_{obs} decreased with an increasing ligand concentration, data were indicative of a rate-limiting conformational change prior to the efficient binding event according to Scheme 1 (*17*):

Scheme 1

$$E \underset{k_{-3}}{\overset{k_3}{\rightleftharpoons}} E^* + L \overset{K_d^*}{\rightleftharpoons} E^*L$$

where L is any ligand. This scheme was used to model glucose, palmitoyl-CoA, and PNP-AMP binding. For this scheme, k_{obs} depends on [L] according to eq 1:

$$k_{obs} = k_3 + k_{-3}\frac{K_d^*}{K_d^* + [L]} \quad (1)$$

In experiments where k_{obs} increased linearly with an increasing ligand concentration (glucose or palmitoyl-CoA), data were fitted to a one-step binding mechanism, according to Scheme 2 and eqs 2 and 3:

Scheme 2

$$E + L \underset{k_{-1}}{\overset{k_1}{\rightleftharpoons}} EL$$

$$k_{obs} = k_1[L] + k_{-1} \quad (2)$$

and

$$K_d = \frac{k_{-1}}{k_1} \quad (3)$$

Both of the paradigms mentioned above can be integrated into Scheme 3,

Scheme 3: Proposed Mechanism of the Interconversion between GK Forms with Glucose Concentration[a]

$$\begin{array}{ccc} E + G & \underset{k\text{-}1}{\overset{k1}{\rightleftharpoons}} & EG \\ {\scriptstyle k\text{-}3}\uparrow\downarrow{\scriptstyle k3} & & {\scriptstyle k\text{-}2}\uparrow\downarrow{\scriptstyle k2} \\ E^* + G & \underset{k\text{-}4}{\overset{k4}{\rightleftharpoons}} & E^*G + ATP \longrightarrow \end{array}$$

[a] E is a super-open form of the enzyme, E* the open form, and G glucose. The closed form of the enzyme with both substrates bound (glucose and ATP) is not represented here.

where G is glucose. In this case, we assumed that measured k_{obs} was reflective of formation of (EG+E*G). Values for the forward (k_3 and k_2) and reverse (k_{-3} and k_{-2}) conformational changes induced by glucose binding can be obtained by fitting the data to eq 4 (*18*):

$$k_{obs} = \frac{k_3 + [G]\frac{k_2}{K_d}}{1 + \frac{[G]}{K_d}} + \frac{k_{-3} + [G]\frac{k_{-2}}{K_d^*}}{1 + \frac{[G]}{K_d^*}} \quad (4)$$

where [G] is the concentration of glucose, $K_d = k_{-1}/k_1$, and $K_d^* = k_{-4}/k_4$. Scheme 3 and eq 4 were used to calculate the parameters for palmitoyl-CoA binding.

Palmitoyl-CoA binding transients were biphasic, and k_{obs} for the second phase hyperbolically increased with the ligand

concentration ([L]). In this case, data could be described by a two-step binding mechanism shown in Scheme 4:

Scheme 4

$$E + L \underset{k_{-1}}{\overset{k_1}{\rightleftharpoons}} EL \underset{k_{-2}}{\overset{k_2}{\rightleftharpoons}} E^*L$$

According to this scheme

$$k_{obs} = \frac{(k_2 + k_{-2})[L]}{K_d + [L]} + k_{-2} \quad (5)$$

where K_d is k_{-1}/k_1 (binding constant for the first step). Since the hyperbolic nature of the curve is indicative of the accumulating EL complex, the final K_d* expression (for the E*L complex), in addition to k_{-2}/k_2, includes a K_d variable.

$$K_d^* = \frac{K_d k_{-2}}{k_2 + k_{-2}} \quad (6)$$

Equilibrium binding data for PNP-AMP were fitted to eq 7 for a hyperbolically increasing one-site binding isotherm:

$$\Delta F = \frac{\Delta F_m[L]}{[L] + K_d} \quad (7)$$

where ΔF_m is the total change in GK fluorescence, [L] is the ligand concentration, and K_d is the dissociation constant. Where fluorescence data showed a sigmoidal dependence, a Hill equation was used to calculate the K_d of the ligand:

$$\Delta F = \frac{\Delta F_m[L]^h}{[L]^h + K_d^h} \quad (8)$$

where h is the Hill coefficient and K_d is an accumulative parameter indicating binding to different conformers.

A separate set of experiments were conducted to probe the glucose dissociation rate by displacement. When two competing ligands, L1 (glucose) and L2 [*N*-acetylglucosamine (NAG)], were tested for their mutual displacement, two potential pathways were evaluated. When enzyme and glucose (E*-L1 and E-L1) in one syringe were mixed with NAG (L2) in the other, a decrease in the magnitude of the signal was observed. The rate of this signal decrease was k_{obs}. Since binding of glucose to the enzyme causes an increase in fluorescence, we hypothesized that NAG was displacing glucose, thus restoring the initial fluorescence (E-L2 complex did not have a distinct signal as tested by mixing enzyme with NAG in an independent experiment). By varying either the NAG concentration in the first syringe and keeping a constant enzyme/glucose mixture in the second syringe or varying the glucose concentration at constant NAG and enzyme concentrations, we measured k_{obs}. This set of data allowed us to probe the rate-limiting step during the ligand displacement and choose the appropriate model.

The mechanism in Scheme 5 predicts that the L1 (glucose) binding-associated conformational change is slow and rate-limiting (*17*):

Scheme 5

$$E^*{-}L1 \underset{k_{-1}}{\overset{k_1}{\rightleftharpoons}} E{-}L1 \overset{K_1}{\rightleftharpoons} E + L1 + L2 \overset{K_2}{\rightleftharpoons} E{-}L2$$

In this mechanism, the expression for the apparent first-order rate constant will be

$$k_{obs} = k_1 \frac{[L1]}{[L1] + K_1\left(1 + \frac{[L2]}{K_2}\right)} + k_{-1} \quad (9)$$

If rate limitation occurs with a conformational change induced by second ligand binding (NAG) according to Scheme 6

Scheme 6

$$E{-}L1 \overset{K_1}{\rightleftharpoons} E + L1 + L2 \overset{K_2}{\rightleftharpoons} E{-}L2 \underset{k_{-1}}{\overset{k_1}{\rightleftharpoons}} E^*{-}L2$$

Then the apparent rate constant is represented by eq 10:

$$k_{obs} = k_1 \frac{[L2]}{[L2] + K_2\left(1 + \frac{[L1]}{K_1}\right)} + k_{-1} \quad (10)$$

In both schemes, K_1 is a K_d for the enzyme−glucose complex and K_2 is a K_d for the enzyme−NAG complex.

RESULTS

Binding of Glucose to the Free Enzyme under Stopped-Flow Conditions. When glucose was rapidly mixed with the free enzyme, an increase in the magnitude of the fluorescence signal was observed, and the transients were fitted to a single-exponential function (Figure 1) to yield an apparent rate constant, k_{obs}. Under our experimental conditions, there was no indication of a double-exponential increase at any glucose concentrations, although biphasic traces have been observed previously for the His-tagged pancreatic GK (*19*). However, when k_{obs} values were plotted against glucose concentration, a clear biphasic dependence could be observed (Figure 2). At low concentrations, the rate decreased exponentially with an increasing glucose concentration but started increasing at concentrations above 3 mM. This unusual behavior suggested that the enzyme in solution exists as a mixture of conformers with different affinities for glucose. To obtain the initial estimates for the parameters, the data were fitted to two separate equations. The initial portion of the curve (up to 3 mM glucose) was modeled to Scheme 1, and the data were fitted to eq 1 to yield a forward isomerization rate (k_3) of 0.4 ± 0.1 s^{-1}, a reverse rate (k_{-3}) of 2.3 ± 0.3 s^{-1}, and a K_d* of 0.06 ± 0.01 mM. At higher concentrations (between 5 and 50 mM), the apparent rate (k_{obs}) increased linearly with an increasing glucose concentration and could be described by either a one-step (Scheme 2) or a two-step binding mechanism, where the intermediate does not accumulate and the transition between the steps is not rate-limiting (*20*). Fitting the data to eqs 2 and 3 gave a k_{on} (k_1) of 5.5 ± 1.3 M^{-1} s^{-1}, a k_{off} (k_{-1}) of 0.4 ± 0.1 s^{-1}, and thus a K_d of 73 ± 18 mM. This value for glucose binding to the low-affinity conformer is close to the reported literature value of 50 mM obtained by simulation according to the gluco-

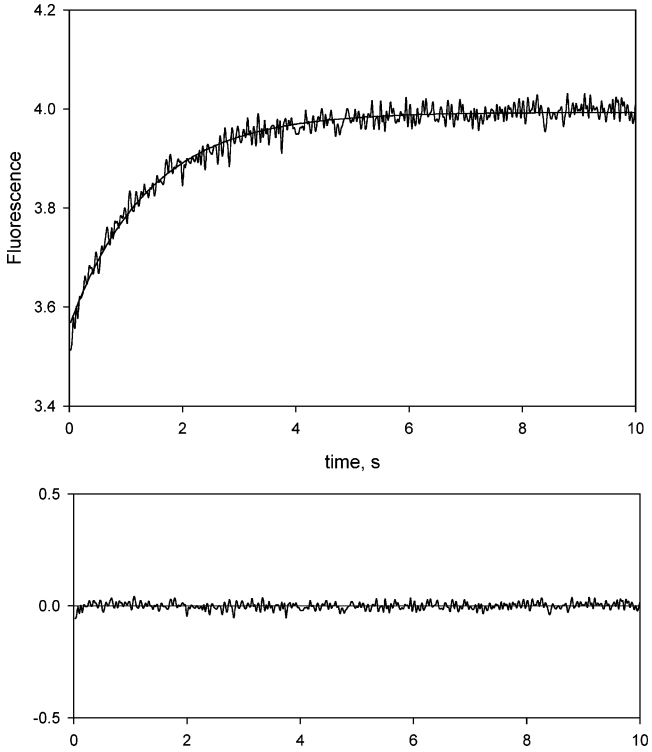

FIGURE 1: Stopped-flow fluorescence time courses for the binding of glucose (50 mM) to glucokinase (1 μM). The bottom panel shows the residuals for the single-exponential fit.

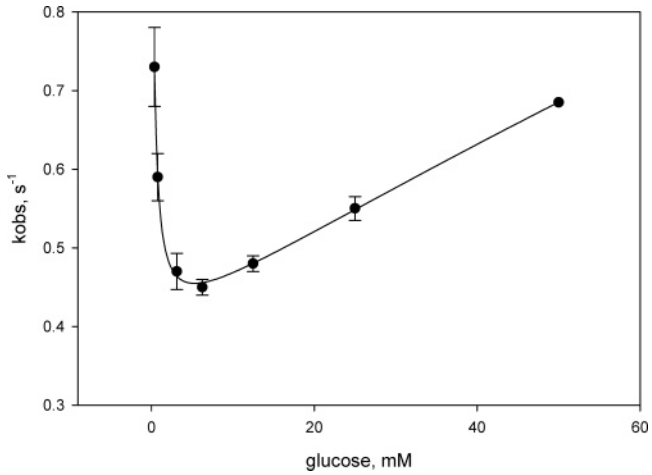

FIGURE 2: Dependence of k_{obs} on glucose concentration. The solid line is a fit to eq 4. The fitted parameters were as follows: $k_3 = 0.3 \pm 0.1$ s^{-1}, $k_2 = 3.4 \pm 0.2$ s^{-1}, $K_d > 100$ mM, $k_{-3} = 1.2 \pm 0.3$ s^{-1}, $k_{-2} = 0.07 \pm 0.01$ s^{-1}, and $K_d^* = 0.17 \pm 0.02$ mM. At each glucose concentration, five to eight curves were recorded and averaged to calculate k_{obs}.

kinase mnemonical reaction mechanism (*21*). The complete set of k_{obs} values was modeled using Scheme 3, which describes the glucose-dependent interconversion of the two enzyme forms. These initial estimates were then used to fit all the data to eq 4. The forward isomerization rates for free enzyme (E) and enzyme complexed with glucose (EG) were 0.3 ± 0.1 (k_3) and 3.4 ± 0.2 s^{-1} (k_2), respectively, and the reverse isomerization rates (k_{-3} and k_{-2}) were 1.2 ± 0.3 and 0.07 ± 0.01 s^{-1} for the free enzyme and the complex, respectively. Unfortunately, the K_d calculated from this equation displayed a high value (>100 mM) and high error,

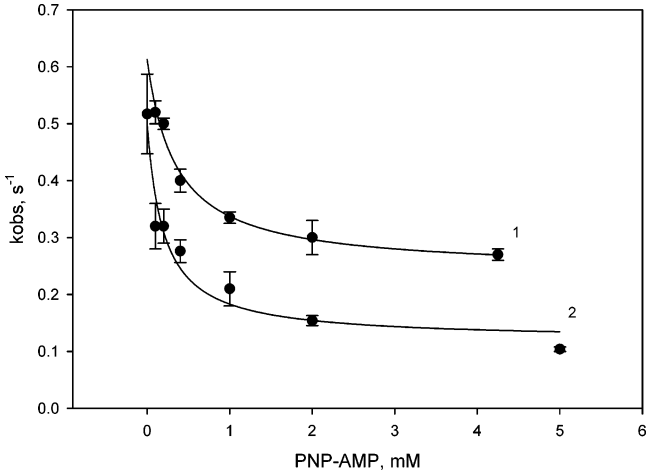

FIGURE 3: Dependence of k_{obs} on PNP-AMP concentration in the presence of 25 (plot 1) or 2 mM glucose (plot 2). Glucose was present in both syringes. Data were fit to eq 1. The fitted parameters at 25 mM glucose were as follows: $k_3 = 0.24 \pm 0.02$ s^{-1}, $k_{-3} = 0.37 \pm 0.03$ s^{-1}, and $K_d^* = 0.35 \pm 0.1$ mM.

since no saturation was observed up to 50 mM glucose and the mechanism described by eq 4 predicts a two-step binding reaction. The calculated K_d^* was 0.17 ± 0.02 mM.

Binding of Glucose in the Presence of PNP-AMP under Stopped-Flow Conditions. When 1 μM glucokinse was mixed with 1 mM PNP-AMP, no significant changes were detected under stopped-flow conditions (in 10 s). However, in the presence of glucose (in both syringes), a single-exponential decrease in fluorescence was observed. The apparent rate constant (k_{obs}) decreased with an increasing PNP-AMP concentration (Figure 3), suggesting that this ligand changes the equilibrium between the GK conformers (complexed with glucose) the same way that glucose does (Scheme 1). The calculated K_d for PNP-AMP (eq 1) at 25 mM glucose was 0.35 ± 0.1 mM, and at 2 mM glucose, the K_d for PNP-AMP was 0.20 ± 0.08 mM. Interestingly enough, the rate of PNP-AMP-induced forward isomerization rate of glucokinase complexed with 25 mM glucose was lower compared to just the glucose-induced isomerization rate (0.24 ± 0.02 s^{-1} in the presence of PNP-AMP and 3.4 ± 0.2 s^{-1} in its absence). However, the reverse isomerization rate was higher compared with the reverse isomerization rate of just the enzyme−glucose complex (0.37 ± 0.03 s^{-1} in the presence of PNP-AMP and 0.07 ± 0.01 s^{-1} in its absence). The accuracy of these experiments was hindered by the low signal amplitude. We, therefore, initiated equilibrium binding studies.

Equilibrium Binding of PNP-AMP. Changes in the intrinsic tryptophan fluorescence of GK upon addition of ligand could be observed under equilibrium conditions as well (Figure 4 A). Titration of GK with glucose resulted in an increasing signal magnitude (curve 2 in Figure 4A), while addition of either PNP-AMP alone (curve 3 in Figure 4A) or PNP-AMP in the presence of glucose (curve 4 in Figure 4A) showed a significant quenching of the protein fluorescence, suggesting that free GK as well as GK complexed with glucose binds the ATP analogue quite well. Titration of free glucokinase with PNP-AMP yielded a clear hyperbolic dependence, and data fitted to eq 7 gave a K_d of 0.23 ± 0.02 mM (Figure 4B). When a similar titration was performed in the presence of 50 mM glucose, a clear sigmoidal dependence was

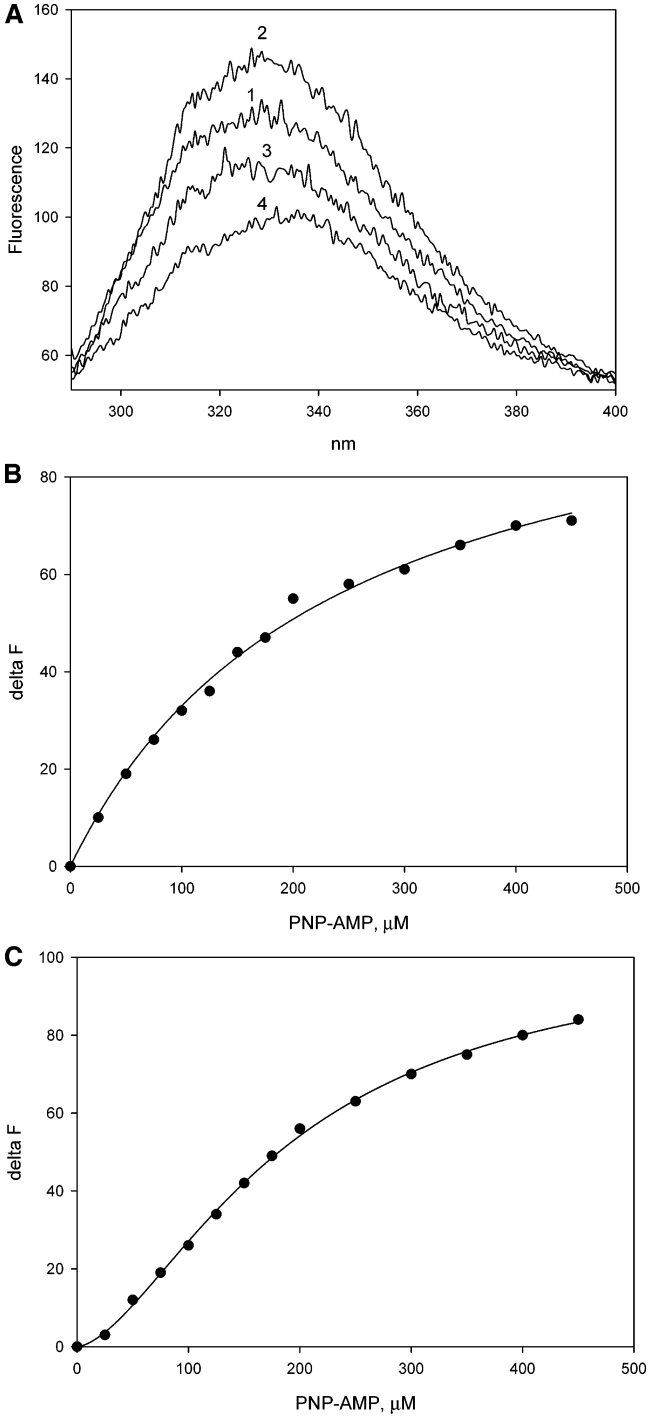

FIGURE 4: Equilibrium titration of glucokinase (1 μM) with PNP-AMP. (A) Spectra of free enzyme (1), enzyme with 20 mM glucose (2), enzyme with added 25 μM PNP-AMP (3), and enzyme with added 20 mM glucose and 200 μM PNP-AMP (4). (B) Dependence of the GK intrinsic fluorescence changes on PNP-AMP concentration. Data were fitted to the eq 7, and the calculated K_d was 0.23 $\pm$ 0.02 mM. (C) Dependence of the glucokinase intrinsic fluorescence changes on PNP-AMP in the presence of 50 mM glucose. Data were fitted to eq 8, and the estimated K_d was 0.190 $\pm$ 0.008 mM, with a Hill slope of 1.6.

observed (Figure 4C), and the data were fitted to eq 8, yielding a K_d of 0.190 $\pm$ 0.008 mM and a Hill slope of 1.6 (Figure 4C).

Transients for Binding of N-Acetylglucosamine (NAG) to GK. In the absence of glucose, we were not able to detect any significant changes in signal under pre-steady state

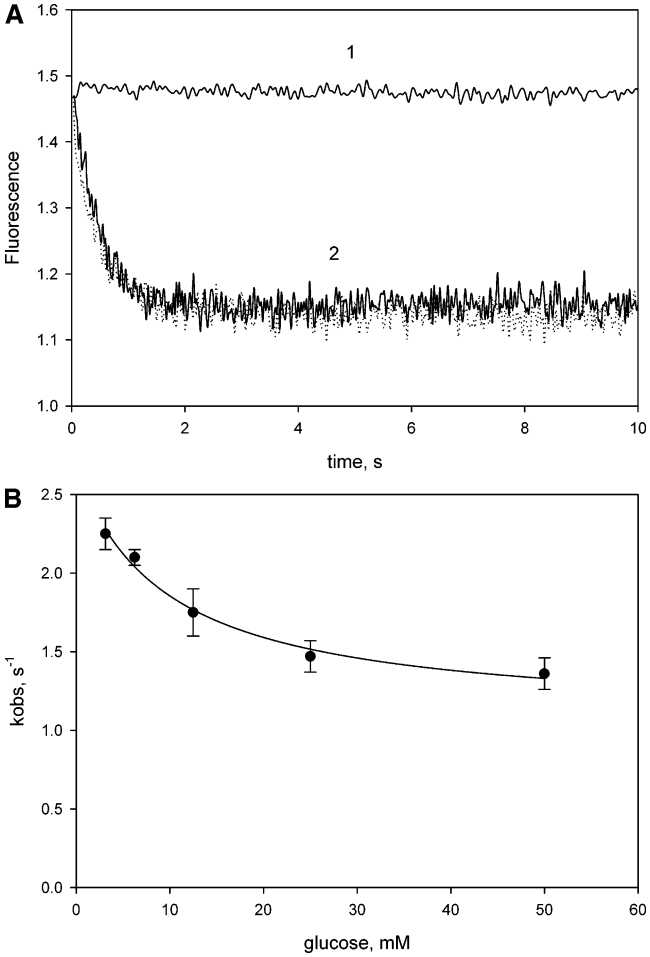

FIGURE 5: (A) Stopped-flow fluorescence time courses of 100 mM NAG binding to glucokinase in the absence (trace 1) and presence of 3 mM glucose (trace 2). (B) Dependence of k_{obs} on glucose concentration in the presence of 100 mM NAG. Data were fitted to eq 10. The estimated parameters were as follows: K_d for NAG (K_2) = 30 $\pm$ 4 mM, K_d for glucose (K_1) = 2.3 $\pm$ 0.3 mM, k_1 = 2 $\pm$ 0.2 s^{-1}, and k_{-1} = 1.1 $\pm$ 0.1 s^{-1}.

conditions up to 100 mM NAG (curve 1 in Figure 5A), but when 3 mM glucose was added to the mixture (in both syringes), a significant decrease in the magnitude of the signal was observed (curve 2 in Figure 5A). Since the signal amplitude was the opposite of that demonstrated by glucose binding, we hypothesized that NAG was displacing glucose from its binding pocket. However, when the NAG concentration was titrated from 10 to 100 mM (in the presence of 3 mM glucose), we observed an increase in k_{obs} (data not shown), suggesting that the K_d for NAG is much higher than the previously reported K_i of 0.24−2 mM (*21*, *22*). To further probe the interaction between glucose and NAG, we titrated glucose in the presence of 100 mM NAG. If glucose binding or dissociation is slow and rate-limiting (Scheme 5), k_{obs} should increase with glucose concentration and decrease with an increasing NAG concentration (eq 9). Our data indicated the opposite, that k_{obs} increased with an increasing NAG concentration (at low glucose concentrations) and decreased with an increasing glucose concentration (Figure 5B). This suggests that NAG binds and dissociates even more slowly than glucose, most likely binding at the same site, but preferentially to a different conformation of glucokinase (Scheme 6). Data were fitted to eq 10, and the K_d for NAG

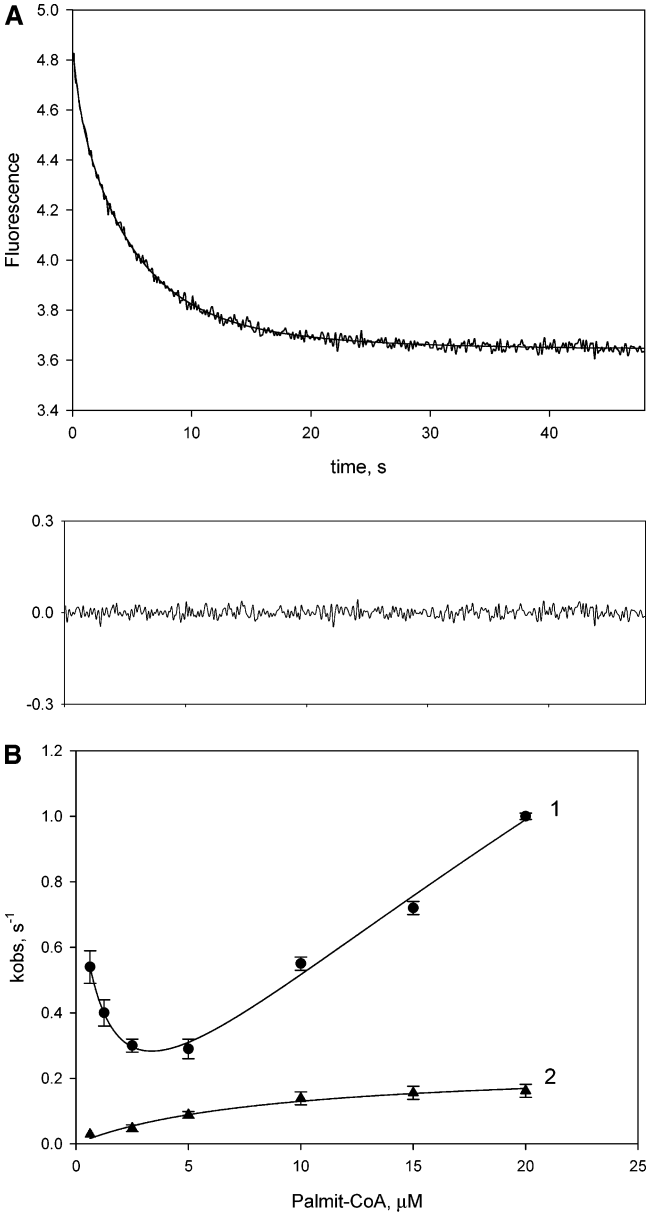

FIGURE 6: (A) Stopped-flow fluorescence transient of 5 μM palmitoyl-CoA binding to glucokinase (0.5 μM) in the presence of 50 mM glucose. The bottom panel shows the residuals for the double-exponential fit. (B) Dependence of k_{obs} of the fast phase (1) and slow phase (2) on palmitoyl-CoA concentration. The line through the points represents a fit to eq 4. Even though the software-derived plot fitted the experimental data points well, the calculated parameters had high errors; therefore, the reported constants are from the fits to eq 1. Fitted parameters for the slow phase (eq 5) were as follows: $k_2 + k_{-2} = 0.24 \pm 0.03$ s^{-1}, $k_{-2} = 0.009 \pm 0.002$ s^{-1}, and $K_d = 9.5 \pm 0.4$ μM.

(K_2) was calculated to be 30 ± 4 mM. k_1 equaled 2 ± 0.2 s^{-1}. k_{-1} equaled 1.1 ± 0.1 s^{-1}. The K_d for the glucose (K_1) was 2.3 ± 0.3 mM. The K_d for glucose is that for the mixture of two conformers and is in good agreement with the value measured from the amplitudes of the stopped-flow transients (K_d = 3 mM) and that reported in the literature in the presence of 5% glycerol (*11*).

Binding of Palmitoyl-CoA under Stopped-Flow Conditions. When palmitoyl-CoA was mixed with GK under stopped-flow conditions in the presence of 50 mM glucose (no Mg^{2+}), clear biphasic transients were observed (Figure 6A). Interestingly, octanoyl-CoA did not exhibit any binding under the same conditions, reconfirming that only long chain acyl-CoAs are ligands for GK (*23*). The k_{obs} values for the fast phase followed the pattern observed for glucose binding: at low concentrations of palmitoyl-CoA, the rate constants were decreasing, and at concentrations above 5 μM, rate constants increased linearly (Figure 6B, plot 1). The k_{obs} values for the slow phase exhibited a hyperbolic dependence on ligand concentration (Figure 6B, plot 2). These data suggest that palmitoyl-CoA binding yields at least two transient complexes with different spectroscopic properties (in equilibrium binding studies, formation of two species was also observed; data not shown). The fast phase data (plot 1 in Figure 6B) could be described by Scheme 3 (or Schemes 1 and 2 to obtain initial estimates) and, when fitted to eq 1, gave values of 0.24 ± 0.03 and 6 ± 2 s^{-1} for the forward (k_3) and reverse (k_{-3}) isomerization rates, respectively. Data were fitted to eqs 2 and 3, resulting in a k_{on} (k_1) of 4.6 × 10^4 M^{-1} s^{-1} and a k_{off} (k_{-1}) of 0.065 s^{-1} and subsequently a K_d of 1.4 μM. Interestingly, this value is close to the K_d we calculated from equilibrium titration studies (data not shown) of 1.6 μM and the apparent inhibition constant reported in the literature of 1.8 μM (*23*). Slow phase data (plot 2 in Figure 6B) exhibited a hyperbolic dependence on palmitoyl-CoA and could be described by Scheme 4. When fitted to eqs 5 and 6, values for $k_2 + k_{-2}$, k_{-2}, and K_d were calculated to be 0.24 s^{-1}, 0.009 s^{-1}, and 9.5 μM, respectively.

DISCUSSION

Mammalian organisms have evolved diverse mechanisms for controlling the rate of glucose phosphorylation depending upon the different needs and metabolic functions of different tissues. In brain and muscle, glucose phosphorylation provides energy; therefore, the rate is controlled by the demand for glucose 6-phosphate. Logically, predominant isozymes in these tissues are hexokinases with characteristically low K_m values for glucose and feedback inhibition by glucose 6-phosphate. In the liver and pancreas, however, the purpose of glucose phosphorylation is to regulate the glucose concentration in the blood. Therefore, the rate of phosphorylation in these tissues depends on the glucose supply rather than the glucose 6-phosphate demand. Not surprising is the fact that liver and pancreatic glucokinase have distinct catalytic and kinetic properties (from the brain and muscle enzyme) to better serve this physiological function. The pronounced positive cooperativity of this monomeric enzyme toward glucose allows it to maintain extremely high sensitivity and responsiveness in the normal physiological glucose range of 2.5−5 mM (*24*, *25*). Storer and Cornish-Bowden (*26*) proposed that this unusual cooperativity for a monomeric enzyme is purely kinetic in origin and can be explained by a "mnemonical" mechanism. Briefly, it requires that free glucokinase exist in two forms that bind glucose with different affinities to give the same catalytically competent enzyme−glucose complex. The cooperativity of glucose binding is reflective of the change in the relative proportions of the two forms of the enzyme that occur as the glucose concentration increases. These two enzyme forms are readily observed in pre-steady state binding experiments (Figure 2), which can be described by Scheme 3. The fast on-rate, high-affinity conformer (E* in Scheme 3) is most likely in a lower proportion. Although this conformer binds glucose better and

Table 1: Microscopic Rate Constants for the Interconversion of the Two GK Forms upon Glucose Binding

	values calculated from eqs 1−3		values calculated from eq 4		simulated parameters using Scheme 3	
	E to E*	EG to E*G	E to E*	EG to E*G	E to E*	EG to E*G
rate for forward isomerization (s^{-1})	0.4 ± 0.1	−	0.3 ± 0.1	3.4 ± 0.2	0.48	4.6
rate for reverse isomerization (s^{-1})	2.3 ± 0.3	−	1.2 ± 0.3	0.07 ± 0.01	1.1	0.06
K_d (mM) (E + G)	73 ± 18		>100		72	
K_d* (mM) (E* + G)	0.06 ± 0.01		0.17 ± 0.02		0.09	

could catalyze phosphorylation faster, it accounts for only a small fraction of the total enzyme, and therefore, its contribution to the total rate is apparently small. Glucose binding eliminates free E* and shifts the equilibrium between the free enzyme forms, E and E*, allowing more E to convert to E*. At low glucose concentrations (until [G] > K_d*), the rate of E*G formation (k_{obs}) is limited by the transition of E to E*, step 3 (decreasing k_{obs} with an increasing glucose concentration). When the glucose concentration is sufficiently high that E* is saturated (>K_d*) and significant binding of glucose to E occurs (transition from EG to E*G is most likely not rate-limiting, since we never observed biphasic traces indicative of EG accumulation), a linear increase in the apparent rate constant is observed. Interestingly, the K_d* calculated for the E*G complex was 0.17 ± 0.01 mM, a value similar to the K_m value for glucose for the cooperativity-devoid hexokinase (*27*). This finding suggests that $S_{0.5}$ (or K_m or $K_{0.5}$) measured in activity experiments is an accumulative parameter reflecting binding of glucose to different affinity conformers, including rate constant(s) for the conformational transition(s). Not surprisingly, the K_d for glucose for each conformer (0.17 and 73 mM) is different from the $S_{0.5}$ measured under steady state conditions (7−10 mM) (*28*, *29*).

To further confirm the proposal for the two conformers, Scheme 3 was used to simulate the glucose binding transients using KINSIM and FITSIM. When initial estimates of the parameters calculated from eq 4 were provided to KINSIM, a good agreement of the theoretical plot with the experimental transient was obtained. The FITSIM-optimized values were in good agreement with those experimentally obtained (Table 1), which reconfirmed the validity of the proposed mechanism. Interestingly, the simulations suggested that only ∼5% of the free enzyme is in the E* conformation.

The rate of the slow conformation change upon glucose binding is much lower than the k_{cat} of 50−60 s^{-1} (*29*), suggesting that this rate limitation must be diminished in the presence of the second substrate, ATP. The pre-steady state binding of the ATP analogue, PNP-AMP, did not reveal significant improvement in the glucose binding parameters (data not shown). We observed a decrease in k_{obs} for PNP-AMP binding (with an increasing PNP-AMP concentrations) at both low and high glucose concentrations (Figure 3). This is consistent with the presence of two enzyme−ligand complexes at equilibrium and interconversion with an increasing ligand concentration (most likely, the EG → E*G transition facilitated by PNP-AMP binding). We could not study product dissociation, since glucose 6-phosphate and ADP were very weak binders (high millimolar range).

These data support the hypothesis proposed by Kamata et al. (*13*) that the enzyme shuttles among at least three conformations: super-open, open, and closed forms. While glucose binding results in a slow transition between the super-open and open forms, the ATP analogue (and possibly ATP) tightens the enzyme from the open to the closed conformation. PNP-AMP binds to the super-open form as well [in the absence of glucose (Figure 4B)] but does not shift it to the open conformer (unless glucose is present). The resulting V_{max} for glucose phosphorylation catalyzed by glucokinase is a subtle interplay between the rates of conformational transitions (including relaxation) caused by substrate binding and product release. It is possible that more than three crystallographically identified forms of GK are present during steady state turnover.

In a further attempt to assess dissociation of glucose and reaction product from the different GK conformers, we probed with *N*-acetylglucosamine (NAG). Special interest in this particular inhibitor was stimulated by the finding that NAG supresses glucose cooperativity (*30*) and maintains a low K_d. It has been suggested that NAG is a competitive inhibitor (with glucose) with a K_i of 0.14−0.24 mM versus glucose (*22*, *30*) and 0.63 mM versus deoxyglucose (*31*). Two competing ligand binding studies allowed us to conclude that even though glucose and NAG might be binding at the same site, they bind preferentially to different GK conformers. The absence of cooperativity with NAG already suggested that this ligand does not bind to the super-open conformation. At high glucose concentrations, the enzyme is predominantly in the open conformation, and it is not surprising that a competitive component between NAG and glucose has been observed (*21*). An increasing glucose concentration affected NAG binding in two opposite (and self-canceling) directions. On the one hand, an increasing glucose concentration was stabilizing more the open form of the enzyme that is available to bind NAG. At the same time, the more GK there is in the open form, the lower the apparent K_d (more enzyme in the high-affinity conformation) and the more difficult it is to displace glucose. Therefore, the slow conformational change associated with NAG binding is most likely reflective of the enzyme transition from the super-open to the open forms (or other as yet crystallographically unidentified enzyme forms).

To understand if these GK conformational changes are controlled only by ligands binding at the active site, we studied binding of palmitoyl-CoA, a reported potent allosteric inhibitor (*16*, *23*). Interestingly enough, we found that even though this ligand binds at a location other than the active site, it is capable of inducing very similar conformational transitions. The biphasic traces observed upon palmitoyl-CoA binding most likely are indicative of ligand binding in a two-step mechanism and yielding complexes with different spectroscopic properties. By analogy to glucose, palmitoyl-CoA binds to both, the super-open and open forms. The difference is that the open form binds palmitoyl-CoA with

Table 2: Effect of Various Ligands on GK Transitions

	NAG[a]	PNP-AMP (with glucose)[b]	PNP-AMP (without glucose)	palmitoyl-CoA (with glucose complex I)[c]	palmitoyl-CoA (with glucose complex II)[d]
forward complex isomerization rate (s^{-1})	2 ± 0.2	0.24 ± 0.02	3.4 ± 0.2	0.24 ± 0.03	0.24 ± 0.01
reverse isomerization rate (s^{-1})	1.1 ± 0.1	0.37 ± 0.03	0.07 ± 0.01	6 ± 2	0.009 ± 0.001
K_d (mM)	30 ± 4	0.35 ± 0.1	0.19 ± 0.01	0.0014 ± 0.0002	0.009 ± 0.001

[a] Results are from data fitting to eq 10. [b] Results are from data fitting to eq 1. [c] Results obtained form the data for the fast phase of the fluorescence transient. Data for k_{obs} were fitted to eq 1. [d] Results obtained from the data for the slow phase of the fluorescence transient. Data for k_{obs} were fitted to eqs 5 and 6.

a sufficiently high affinity for the EL complex (analogous to EG in Scheme 3) to accumulate as demonstrated by the hyperbolic k_{obs} dependence of the slower phase (Figure 6B, plot 2). Interestingly, this ligand is a reported inhibitor, meaning that it decreases the apparent GK activity either by increasing the K_m of the substrate (apparent competitive inhibitor) or by a combination of increasing the K_m and decreasing the k_{cat} (mixed-type inhibitor). Even though it was reported that palmitoyl-CoA is affecting only the K_m for glucose (without altering the Hill coefficient) (*23*), these conclusions were made on the basis of Dixon plots, which, when nonlinear, do not give unambiguous answers. We anticipate that this inhibitor could potentially bind to the super-open conformation (E in Scheme 3) and thus stabilize more of the low-affinity conformer. In kinetic studies, this would result in an increased K_m for glucose. Additional binding of palmitoyl-CoA to the open form would allow the enzyme to maintain the same Hill coefficient (indicative of a transition between the two forms) without affecting k_{cat} too much. These data suggest that other molecules binding at the allosteric site(s) would impact GK transitions in a manner similar to that of the active site ligands.

All kinetic parameters for these diverse ligand binding are presented in Table 2. The data suggest that even though ligands bind to different sites, they all affect GK by inducing transitions and most likely altering the ratio between the different conformers.

Glucokinase kinetic properties have been studied for more than three decades. Steady state analysis of the enzyme's kinetic mechanism in a coupled assay is complicated by multiple factors. This enzyme demonstrates cooperativity with glucose which is dependent on ATP concentration. During the reaction, the concentration of various inhibitory ionic species changes depending on the ratio of the reagents and pH (ATP^{4-}, Mg^{2+}, ADP^{3-}, and $MgADP^{-}$) (*26*, *32*), and other factors interfering with GK activity (unpublished data). It is not surprising that a set of diverse conclusions have been presented and supported by different authors. In this study, we chose to isolate binding steps from catalysis and thus were able to provide strong evidence of the previously implied, but never demonstrated, preexisting equilibrium of two free enzyme conformers: the super-open and open forms (*13*, *21*, *26*). This phenomenon underlying enzyme cooperativity and the resulting glucose sensing capacity are extremely important in identifying suitable antidiabetic agents. On the basis of the mechanism discussed here, one could argue that ligands which stabilize GK allosterically in a low-affinity conformation (manifested by a low K_m and a Hill slope of unity) might not be the most desirable agents.

ACKNOWLEDGMENT

We are grateful to Dr. Alan Rendina for the most valuable discussions during the course of this work and Drs. Archie Argyrou, Jeane Whaley, Mark Kirby, Cynthia Gates, and Simeon Taylor for reading the manuscript and valuable comments.

REFERENCES

1. Matschinsky, F. M. (1990) Glucokinase as glucose sensor and metabolic signal generator in pancreatic β-cells and hepatocytes, *Diabetes 39*, 647−652.
2. Postic, C., Shiota, M., Niswender, K. D., Jetton, T. L., Chen, Y., Moates, J. M., Shelton, K. D., Linder, J., Cherrington, A. D., and Magnuson, M. A. (1999) Dual roles for glucokinase in glucose homeostasis as determined by liver and pancreatic β-cell specific gene knockouts using Cre recombinase, *J. Biol. Chem. 274*, 305−315.
3. Shiota, M., Postic, C., Fujimoto, Y., Jetton, T. L., Dixon, K., Pan, D., Grimsby, J., Grippo, J. F., Magnuson, M. A., and Cherrington, A. D. (2001) Glucokinase gene locus transgenic mice are resistant to the developement of obesity-induced type 2 diabetes, *Diabetes 50*, 622−629.
4. Niswender, K. D., Postic, C., Jetton, T. L., Bennett, B. D., Piston, D. W., Efrat, S., and Magnuson, M. A. (1997) Cell-specific expression and regulation of a glucokinase gene locus transgene, *J. Biol. Chem. 272*, 22564−22569.
5. Vionnet, N., Stoffel, M., Takeda, J., Yasuda, K., Bell, G. I., and Zouali, H. (1992) Nonsense mutation in the glucokinase gene causes early onset non-insulin-dependent diabetes mellitus, *Nature 356*, 721−722.
6. Froguel, P., Zouali, H., Vionnet, N., Vehlo, G., Vaxillaire, M., Sun, F., Lesage, S., Stoffel, M., Takeda, J., Passa, P., Permutt, M. A., Beckman, J. S., Bell, G. I., and Cohen, D. (1993) Familial hyperglycemia due to mutations in glucokinase. Definition of subtype of diabetes melittus, *N. Engl. J. Med. 328*, 697−702.
7. Glasser, B., Kesavan, P., Heyman, M., Davis, E., Cuesta, A., and Buchs, A. (1998) Familial hyperinsulinism caused by an activating glucokinase mutation, *N. Engl. J. Med. 338*, 226−230.
8. Grimsby, J., Sarabu, R., Corbett, W. L., Haynes, N.-E., Bizzarro, F. T., Coffey, J. W., Guertin, K. R., Hilliard, D. W., Kester, R. F., Mahaney, P. E., Marcus, L., Qi, L., Spence, C. L., Tengi, J., Magnuson, M. A., Chu, C. A., Dvorozniak, M. T., Matschinsky, F. M., and Grippo, J. F. (2003) Allosteric Activators of Glucokinase: Potential Role in Diabetes Therapy, *Science 301*, 370−373.
9. Efanov, A. M., Barrett, D. G., Brenner, M. B., Briggs, S. L., Delaunois, A., Durbin, J. D., Giese, U., Guo, H., Radloff, M., Gil, G. S., Sewing, S., Wang, Y., Weichert, A., Zaliani, A., and Gromada, J. (2005) A Novel Glucokinase Activator Modulates Pancreatic Islet and Hepatocyte Function, *Endocrinology 146*, 3696−3701.
10. McKerrecher, D., Allen, J. V., Caulkett, W. R., Donald, C. S., Fenwick, M. L., Grange, E., Johnson, K. M., Jones, C. D., Pike, K. G., Rayner, J. W., and Walker, R. P. (2006) Design of a potent, soluble glucokinase activator with excellent in vivo efficacy, *Bioorg. Med. Chem. Lett. 16*, 2705−2709.
11. Lin, X.-S., and Neet, K. E. (1990) Demonstration of a slow conformational change in liver glucokinase by fluorescence spectroscopy, *J. Biol. Chem. 265*, 9670−9675.

12. Neet, K. E., Keenan, R. P., and Tippet, P. S. (1990) Observation of a kinetic slow transition in monomeric glucokinase, *Biochemistry 29*, 770−777.
13. Kamata, K., Mitsuya, M., Nishimura, T., Eiki, J., and Nagata, Y. (2004) Structural basis for allosteric regulation of the monomeric allosteric enzyme human glucokinase, *Structure 12*, 429−438.
14. Mookhtiar, K. A., Kalinowski, S. S., Brown, K. S., Tsay, Y. H., Smith-Monroy, C., and Robinson, G. W. (1996) Heterologous expression and characterization of rat liver glucokinase regulatory protein, *Diabetes 45*, 1670−1677.
15. Lange, A. J., Xu, L. Z., Van Poelwijk, F., Lin, K., Granner, D. K., and Pilkis, S. J. (1991) Expression and site-directed mutagenesis of hepatic glucokinase, *Biochem. J. 277*, 159−163.
16. Tippett, P. S., and Neet, K. E. (1982) Specific inhibition of glucokinase by long chain acyl coenzymes A below the critical micelle concentration, *J. Biol. Chem. 257*, 12839−12845.
17. Auzat, I., Gawlita, E., and Garel, J.-R. (1995) Slow ligand-induced transitions in the allosteric phosphofructokinase from *Escherichia coli*, *J. Mol. Biol. 249*, 478−492.
18. Masson, P., Schopfer, L. M., Froment, M. T., Debouzy, J. C., Nachon, F., Gillon, E., Lockridge, O., Hrabovska, A., and Goldstein, B. N. (2005) Hysteresis of butyrylcholinesterase in the approach to steady-state kinetics, *Chem.-Biol. Interact. 157−158*, 143−152.
19. Heredia, V. V., Thompson, J., Nettleton, D., and Sun, S. (2006) Glucose-induced conformational changes in glucokinase mediate allosteric regulation: Transient kinetic analysis, *Biochemistry 45*, 7553−7563.
20. Morrison, J. F., and Stone, S. R. (1985) Approaches to the study and analysis of the inhibition of enzymes by slow-and tight binding inhibitors, *Comments Mol. Cell. Biophys. 2*, 347−368.
21. Moukil, M. A., and Van Shaftingen, E. (2001) Analysis of the cooperativity of human β-cell glucokinase through the stimulatory effects of glucose on fructose phosphorylation, *J. Biol. Chem. 276*, 3872−3878.
22. Moukil, M. A., Veiga-da-Cuhna, M., and Van Scheftingen, E. (2000) Study of the regulatory properties of glucokinase by site-directed mutagenesis, *Diabetes 49*, 195−201.
23. Tippett, P. S., and Neet, K. E. (1982) An allosteric model for the inhibition of glucokinase by long chain acyl coenzyme A, *J. Biol. Chem. 257*, 12846−12852.
24. Storer, A., and Cornish-Bowden, A. (1976) Kinetics of rat liver glucokinase. Co-operative interactions with glucose at physiologically significant concentrations, *Biochem. J. 159*, 7−14.
25. Matschinsky, F. M., Magnuson, M. A., Zelent, D., Jetton, T. L., Doliba, N., Han, Y., Taub, R., and Grimsby, J. (2006) The network of glucokinase-expressing cells in glucose homeostasis and the potential of glucokinase activators for diabetes therapy, *Diabetes 55*, 1−12.
26. Storer, A., and Cornish-Bowden, A. (1977) Kinetic evidence for a "mnemonical" mechanism for rat liver glucokinase, *Biochem. J. 165*, 61−69.
27. Sebastian, S., Wilson, J. E., Mulichak, A., and Garavito, R. M. (1999) Allosteric regulation of type I hexokinase: A site-directed mutational study indicating location of the functional glucose-6-phosphate binding site in the N-terminal half of the enzyme, *Arch. Biochem. Biophys. 362*, 203−210.
28. Xu, L. Z., Harrison, R. W., Weber, I. T., and Pilkis, S. J. (1995) Human β-cell glucokinase, *J. Biol. Chem. 270*, 9939−9946.
29. Davis, E. A., Cuesta-Munoz, A., Raoul, M., Sweet, I., Moates, M., Magnuson, M. A., and Matchinski, F. M. (1999) Mutants of glucokinase cause hypoglycemia and hyperglycemia syndromes and their analysis illuminates fundamental quantitative concepts of glucose homeostasis, *Diabetologia*, 1175−1186.
30. Cardenas, M. L., Rabajille, E., and Niemeyer, H. (1984) Suppression of kinetic cooperativity of hexokinase D (glucokinase) by competitive inhibitors, *Eur. J. Biochem. 145*, 163−171.
31. Monasterio, O., and Cardenas, M. L. (2003) Kinetic studies of rat liver hexokinase D (glucokinase) in non-cooperative conditions show an ordered mechanism with MgADP as the last product to be released, *Biochem. J. 371*, 29−38.
32. Storer, A., and Cornish-Bowden, A. (1976) Concentration of $MgATP^{2-}$ and other ions in solution, *Biochem. J. 159*, 1−5.

BI0617308